
Original Article

Topical Application of Nano-chitin Accelerates Wound Healing in Diabetic Mice

Yuka Kaneko *

Department of Dermatology,
Kyoto Prefectural University of Medicine Graduate School of Medical Science

Abstract

Chitin is the second most abundant natural mucopolysaccharide with prominent biocompatibility. In fabric form, it is clinically used as wound dressing material in Japan (Beschitin[®], Nipro Corporation). Soluble nanocrystal chitin (nano-chitin) was generated and evaluated its potential as a wound dressing material using a murine impaired diabetic wound healing model. Nano-chitin significantly accelerated granulation tissue formation, with notable increases in angiogenesis and inflammatory cell infiltration. Nano-chitin showed the same effect on wound closure as Beschitin[®], which contained a three times higher chitin concentration than that of nano-chitin. *In vitro*, the impact of nano-chitin on THP-1 cells was evaluated by PCR and proliferation assay. Nano-chitin directly promoted vascular endothelial growth factor, tumour necrosis factor- α , and interleukin-1 expression while not inhibiting cell growth in THP-1 cells, which are essential in promoting granulation tissue formation. This suggests that the favourable effects of nano-chitin on wound healing are due to its direct influence on inflammatory cells. In conclusion, gelatinous nano-chitin that promoted wound healing in diabetic mice was successfully generated. This study would be the first to evaluate the direct mechanisms underlying the effects of chitin on wound healing *in vitro*.

Key Words: Chitin, Nanomedicine, Wound healing.

Introduction

Chitin is the second most abundant natural mucopolysaccharide contained in the shells of crustaceans, exoskeletons of insects, cell walls of fungi, and cuttlebones of squids.¹⁾ Since chitin is prominently biocompatible, the fabric form of chitin is clinically used as a wound dressing mate-

rial in Japan (Beschitin[®], Nipro Corporation, Osaka, Japan). The favourable effects of chitin dressing on wound healing are thought to promote the production of growth factors from inflammatory cells and retain adequate moisture in wounds.²⁾ Furthermore, chitin has been expected and attempted to be applied extensively in the fields of agriculture,^{3) 4)} food industry,^{5) 6)} tissue

Received: January 26, 2022. Accepted: June 30, 2022

* Correspondence: Yuka Kaneko Department of Dermatology, Kyoto Prefectural University of Medicine Graduate School of Medical Science, 465, Kajii-cho, Kawaramachi-Hirokoji, Kamigyo-ku, Kyoto 602-8566, Japan

y-kaneko@koto.kpu-m.ac.jp

doi:10.32206/jkpum.131.09.751

engineering,⁷⁾ and material sciences.⁸⁾ However, owing to its firm crystalline structure, which is insoluble and hard to process, the development has been very slow. To overcome these limitations to chitin applications, converting its insoluble crystalline structure into an easily processable form is important. In addition, impaired wound healing is one of the major clinical problems in patients with diabetes.⁹⁾ Impaired wound healing in diabetes is characterised by delayed cellular infiltration, impaired angiogenesis, and diminished granulation tissue formation; it is partly caused by cellular dysfunction and impairment of growth factor production.^{9,13)} A nanocrystal form of chitin (nano-chitin) that could become gelatinous upon mixing with water was generated, and evaluated its therapeutic potential as a new wound dressing material using a murine impaired diabetic wound healing model. I further assessed the mechanisms of chitin-mediated promotion of wound healing *in vitro* using the THP-1 human monocyte cell line, which is a major inflammatory cell line.

Materials and methods

Animals

All protocols were approved by the Institutional Animal Care and Use Committee of the Kyoto Prefectural University of Medicine. Genetically diabetic C57BLKS/J-m^{+/+}Lepr^{db} mice (db/db mice) were obtained from Clea Japan, Inc. (Tokyo, Japan).

Preparation of nano-chitin

Nano-chitin was produced from alkaline chitin dope (amorphous chitin) by neutralisation at low temperature with low deacetylation and depolymerisation of chitin. Briefly, 50 g of powdered chitin was diluted in 500 ml of NaOH (48% w/w) and maintained for 24 h at room temperature. Next, 1,000 g of crushed ice was added to amorphous chitin to keep it at a low temperature (-10 to -15 °C) and gently stirred until the ice

melted completely. An additional 500 g of crushed ice and 12 N HCl were added to neutralise the mixture to pH 6.5-7.5. During neutralisation, chitin was precipitated in the nanocrystal form (nano-chitin). After the solid-liquid separation followed by removal of NaCl by washing with distilled water, nano-chitin was dehydrated until it became gelatinous. The concentration of the gelatinous nano-chitin was adjusted to 3.0%. Beschitin® was photographed using a scanning electron microscope (SU5000, Hitachi High-Tech Science, Tokyo, Japan). Nano-chitin was photographed using a transmission electron microscope (JEM-2100, JEOL Ltd., Tokyo, Japan).

Wound creation

The mice were 8 weeks old; the mean body weight is 34.1g and the mean plasma glucose level is 418mg/dl at the time of the study. Briefly, after induction of deep anaesthesia by intraperitoneal injection of a mixture of medetomidine chloride (3 mg/kg), midazolam (4 mg/kg), and butorphanol tartrate (5 mg/kg), full-thickness excisional skin wounds were made on the backs of the mice using 8-mm skin biopsy punches. A circular silicone splint (inner diameter of 10 mm and outer diameter of 20 mm) (Grace Bio-Labs, Bend, Oregon, USA) was placed around each wound. Each wound was covered with semipermeable polyurethane dressing (OpSite®, Smith and Nephew, Massillon, OH, USA) after topical application of 100 µl of 3% nano-chitin (containing 3 mg nano-chitin) or vehicle (distilled water: 100 µl). Nano-chitin or vehicle was applied on days 0, 4, and 7 after wounding.

Similarly, full-thickness excisional skin wounds were made on the backs of mice using 8-mm skin biopsy punches. A circular silicone splint (inner diameter of 10 mm and outer diameter of 20 mm) (Grace Bio-Labs) was placed around each wound. Each wound was covered with semipermeable polyurethane dressing

(OpSite®, Smith and Nephew) after topical application of 100 μ l of 3% nano-chitin (3 mg) or Beschitin® W-A (Nipro Corporation). Beschitin® was cut in a circular shape, with each particle 8 mm in diameter and approximately 9.5 mg in weight.

Monitoring of wound closure and granulation tissue formation

Wound closure was monitored by capturing images using a digital camera (RICOH G800, RICOH, Tokyo, Japan) on days 0, 4, 7, and 10 after wounding. The images were analysed using ImageJ software version 1.51 (NIH, Bethesda, MD, USA) by tracing the wound margin using a high-resolution computer mouse and calculating the pixel area. Then, the wound areas were compared using Student's t-test.

To evaluate the degree of granulation tissue formation, wound tissues were harvested on day 7 after euthanising mice. The tissue samples were divided in half at the maximum cut surface, fixed in 10% formalin, and processed using regular histopathological methods. The tissue sections were stained with hematoxylin and eosin. The sections were then analysed using ImageJ software version 1.51 (NIH) by tracing the granulation tissue margin using a high-resolution computer mouse and calculating the pixel area. Then, the wound areas were compared using Student's t-test.

Immunostaining for evaluation of inflammation and vascularity

For evaluation of inflammation and vascularity during wound healing, the densities of inflammatory cells and vascular structures were determined using immunostaining. On day 7, wound tissues were harvested after euthanising mice. The tissue samples were divided in half at the maximum cut surface and then fixed with formalin and embedded in paraffin. The sections were deparaffinised, and antigen retrieval treatment was per-

formed by heating to 121 °C for 10 min. The sections were then incubated overnight at 4 °C with the anti-mouse endothelial cell marker CD31 (PECAM) rat monoclonal antibody (1:300; Dianova, Hamburg, Germany), anti-mouse F4/80 rat monoclonal antibody (1:250; BMA BIOMEDICALS, Augst, Switzerland), and anti-mouse Ly6g rat monoclonal antibody (1:100; Abcam, Cambridge, UK). Next, the sections were incubated for 30 min at 23 °C with the secondary antibody HISTOFINE simple stain MAX-PO (Rat) (Nichirei, Tokyo, Japan). For each slide, five different granulation tissue fields were selected and captured. The CD31 + cells, F4/80 + cells, and Ly6g + cells were counted at 400-fold magnification.

Cell preparation and culture

The THP-1 cell line was obtained from the European Collection of Cell Cultures (DS PHARMA BIOMEDICAL, Osaka, Japan) and maintained in RPMI-1640 medium containing 10% non-heat-inactivated fetal bovine serum and 1% antibiotic/anti-mycotic solution (both from GIBCO, Carlsbad, CA, USA) at 37 °C in 5% CO₂. The cells were resuspended at 3×10^5 cells/ml in RPMI-1640 medium containing 10% heat-inactivated fetal bovine serum and 1% antibiotic/anti-mycotic solution, which was supplemented with nano-chitin at various concentrations (0 μ g/ml, 0.3 μ g/ml, 3 μ g/ml, and 30 μ g/ml).

Quantitative real-time reverse transcription-polymerase chain reaction (RT-PCR)

For the *in vitro* studies, THP-1 cells were cultured in the presence of various doses of nano-chitin (0, 0.3, 3, and 30 μ g/ml). The cells were harvested after 6, 12, and 24 h, and RNA was extracted using ISOGEN II (#311-07361, NIPPON GENE, Tokyo, Japan) according to the manufacturer's instructions. Total RNA was reverse-transcribed using the iScript cDNA

Synthesis Kit (Bio-Rad, Hercules, CA, USA). The cDNA was amplified on the StepOne thermal cycler (Applied Biosystems, Foster City, CA, USA) using the following primers and probes: vascular endothelial growth factor (VEGF) - forward: 5'-AAGTCCACAGAAATGCTTGTTAA AAG-3' and VEGF-reverse: 5'-GTTCGTACATG GCCGTCTGTAA-3'; Interleukin (IL) -1-forward: 5'-GGTGTCTCCATGTCCTTTG-3' and IL-1-reverse: 5'-GGATCTACACTCTCCAGCTG-3'; tumour necrosis factor (TNF) - α -forward: 5'-AAGCCTGTAGCCCATGTTGTA-3' and TNF- α -reverse: 5'-TCAGCTCCACGCCATTG-3'; and 18S-forward: 5'-GAAACGGCTACCACATCCAAG-3' and 18S-reverse: 5'-CGGGTCGGGAGTGGGT-3'. Additionally, THP-1 cells were cultured in the presence of nano-chitin (0,30 μ g/ml) or medium with vehicle. The cells were harvested after 6h, and RNA was extracted using ISOGEN II (#311-07361, NIPPON GENE, Tokyo, Japan) according to the manufacturer's instructions. Total RNA was reverse-transcribed using the iScript cDNA Synthesis Kit (Bio-Rad, Hercules, CA, USA). The cDNA was amplified on the StepOne thermal cycler (Applied Biosystems, Foster City, CA, USA) using the following primers and probes: IL-6-forward: 5'-CCACCGGGAACGAAAGAGAA-3' and IL-6-reverse: 5'-TGGGGGTATTGTGGAGAA GGA-3'; IL-8-forward: 5'-ACACTGCGCAACAC AGAAATTA-3' and IL-8-reverse: 5'-TTTGCTTG AAGTTTCACTGGCAT-3'; epidermal growth factor (EGF) -forward: 5'- AGTGCATCAACA CCGAAGGT-3' and EGF-reverse: 5'-CCCCAGTT GGCATCATCAA-3'; b fibroblast growth factor (FGF) -forward: 5'- TCTTCCTGCGCATCCACC-3' and bFGF-reverse: 5'- TAGCTTGATGTGAGG GTCGC-3'; and 18S-forward: 5'-GAAACGGCTA CCACATCCAAG-3' and 18S-reverse: 5'-CGGG TCGGGAGTGGGT-3'. The expression of the target gene mRNAs was calculated using the comparative C_T method, as previously described,¹⁴⁾ with normalisation to the expression

of the control 18S rRNA. Differences in C_T values were calculated for each target mRNA by taking the mean value for duplicate reactions and subtracting the mean value for 18S rRNA. The fold change in the expression of each target gene in the treated cells relative to that in the control cells was calculated as: relative expression = $2^{-\Delta CT}$.

Cell proliferation assay

THP-1 cells cultured in RPMI-1640 medium were suspended in 96-well plates and cultured for 24 h. Nano-chitin was then added to the medium at various concentrations (0, 0.3, 3, and 30 μ g/ml). Cell Counting Kit-8 reagent (Dojindo, Kumamoto, Japan) was added to the wells 6, 12, and 24 h after nano-chitin administration, and incubation was continued for an additional 3 h at 37 °C. After incubation, A_{450} of the cell cultures was measured, and cell viability was calculated using the formula: $[(A_{test} - A_{background}) / (A_{control} - A_{background})] \times 100$, where A is the absorbance at A_{450} ; background refers to the medium alone, and control refers to the untreated cell population.

Statistical analysis

All results are presented as mean \pm standard error of the mean. Statistical comparisons between two groups were performed using Student's t -test, and analysis of variance was used for serial analysis, with $P < 0.05$ being considered to indicate statistical significance. All *in vitro* experiments were performed at least three times.

Results

Preparation of nano-chitin

The nanocrystal form of chitin was produced from amorphous chitin. Compared with Beschitin[®], a fabric form of chitin, nano-chitin was gelatinous and water-soluble (Fig. 1a). Electron microscopic examination revealed that Beschitin[®] had a fibrous structure with a diameter of 100 μ m, whereas nano-chitin was an amor-

phous nano-particle whose diameter was less than 10 nm (Fig. 1b). The nano-chitin was more than 1,000 times smaller than Beschitin®.

Nano-chitin accelerates wound healing in diabetic mice

To investigate the effect of nano-chitin on wound closure, full-thickness skin wounds were created on the dorsal skin of db/db mice and applied nano-chitin or vehicle every 3 days. Wound areas on days 0, 4, and 7 in nano-chitin- or vehicle-treated diabetic mice are shown in Fig. 2a. On days 4 and 7 after the creation of the wound, the areas of the wounds in the topical nano-chitin group were significantly reduced compared with those in the vehicle group ($n = 3$ per group, $*P < 0.05$, $**P < 0.001$ vs. vehicle). However, after 10 days, the difference tended to decrease (Fig. 2b).

Hematoxylin and eosin staining showed thick granulation tissue formation and re-epithelialisation in the nano-chitin-treated wounds,

whereas thin granulation tissue was formed in the vehicle-treated wounds (Fig. 2c). The area of granulation tissue (black broken lines) in nano-chitin-treated wounds was significantly larger than that in the vehicle-treated wounds ($*P < 0.05$ vs. vehicle) (Fig. 2d).

Nano-chitin treatment increases inflammation and neovascularisation

Since wound healing requires the induction of inflammation and formation of new blood vessels, the vascularity and inflammation of the wound granulation tissue were next evaluated. Wound angiogenesis was analysed using CD31 immunostaining of 10- μ m frozen wound sections. Inflammation was analysed using Ly6g and F4/80 immunostaining to visualise the inflammatory cell neutrophils and macrophages, respectively. CD31, Ly6g, and F4/80 immunostainings of wound granulation tissue on day 7 are shown in Fig. 3. Topical application of nano-chitin significantly enhanced wound vascularity and neu-

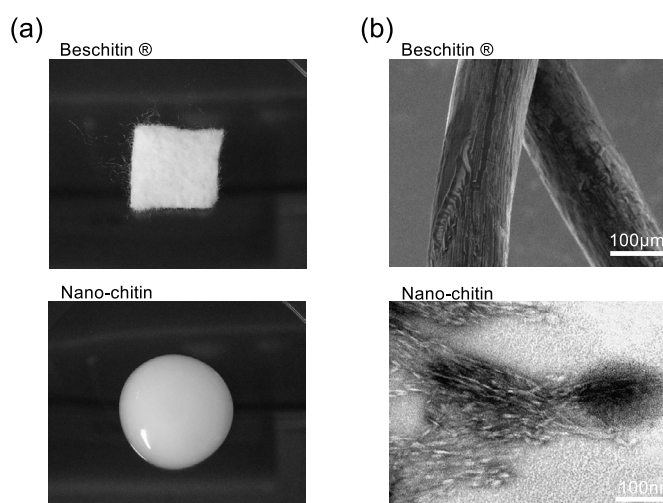


Figure 1. Beschitin® and nano-chitin. (a) Macroscopic presentation of Beschitin® and nano-chitin. Beschitin® is a fabric with an unsolvable structure, whereas nano-chitin is gelatinous and has a water-soluble structure. (b) Electron microscopic images of Beschitin® and nano-chitin. Beschitin® was photographed using a scanning electron microscope (Scale bar = 100 μ m). Nano-chitin was photographed using a transmission electron microscope (Scale bar = 100 nm).

trophil infiltration. Macrophage infiltration tended to be increased, albeit not significantly ($n = 5$ per group, $*P < 0.05$ vs. vehicle).

Nano-chitin upregulates VEGF, IL-1, TNF- α , IL-8, and bFGF in THP-1 cells

To elucidate the mechanisms responsible for the effects of chitin, the VEGF, TNF- α , and IL-1 mRNA levels *in vitro* were evaluated. THP-1 cells

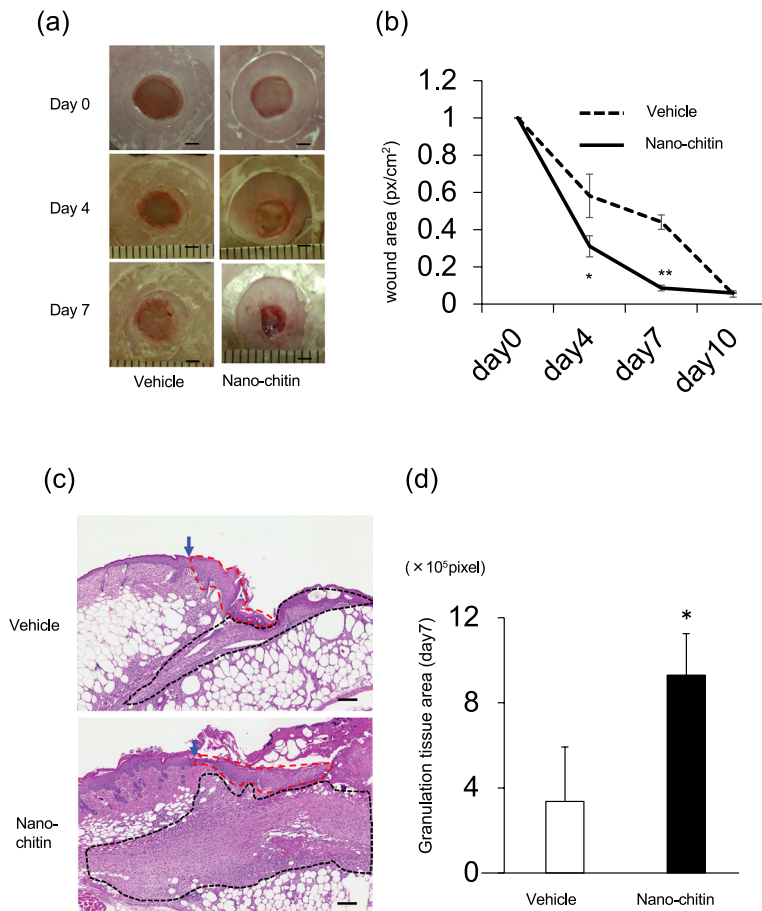


Figure 2. Clinical effect of nano-chitin on full-thickness skin wounds in db/db mice. (a) Representative macroscopic appearance of the wound healing process in the two treatment groups (left panels; vehicle, right panels; nano-chitin). Scale bar = 2 mm. (b) The percentage of the wound area. On days 4 and 7, nano-chitin significantly accelerated wound closure compared with the vehicle ($n = 3$ per group, $*P < 0.05$, $**P < 0.001$ vs. control). (c) Hematoxylin and eosin-stained histological images of the ulcer samples in the indicated groups. The black broken lines indicate the areas of granulation tissue, and the broken red lines indicate the neopithelium. Blue arrows indicate the original wound edge. In the vehicle group, the wound bed showed a thin layer of granulation tissue over the adipose tissue. In contrast, a thick layer of granulation tissue was observed in the nano-chitin-treated group. (Scale bar = 500 μ m.) (d) Granulation tissue areas of sections were analysed using ImageJ software version 1.51 (NIH) by tracing the granulation tissue margin using a high-resolution computer mouse and calculating the pixel area. The nano-chitin-treated group had larger granulation tissue areas than the vehicle-treated group ($n = 5$ per group, $*P < 0.05$ vs. control).

were harvested for 2 days and assessed for VEGF, TNF- α , and IL-1 mRNA levels using quantitative real-time RT-PCR. The upregulation of VEGF (Fig. 4A a), TNF- α (Fig. 4A b), and IL-1 (Fig. 4A c) in chitin-treated wounds was higher than that in saline-treated wounds (n = 3 per group, * P <

0.05, ** P < 0.001 vs. control). In addition, VEGF (Fig. 4B d), TNF- α (Fig. 4B e), and IL-1 (Fig. 4B f) expression decreased with time (n = 3 per group, * P < 0.05, ** P < 0.001 vs. control). Additionally, the IL-6, IL-8, EGF, and bFGF mRNA levels *in vitro* were evaluated. The upregu-

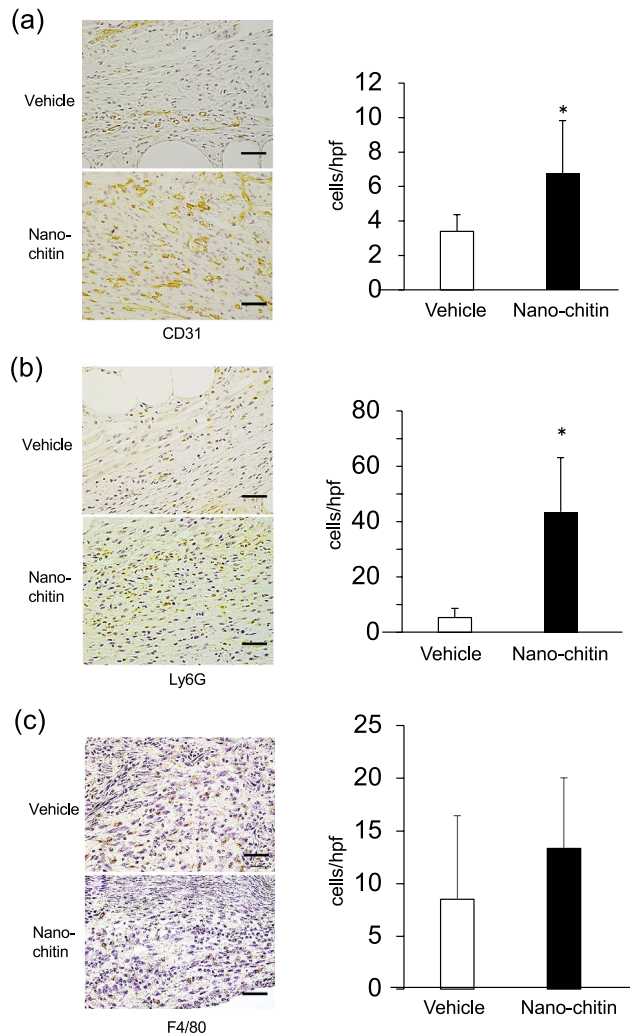


Figure 3. Effects of topical application of nano-chitin on angiogenesis and inflammatory cell infiltration in wound granulation tissues. Immunohistochemical staining of CD31 (a), Ly6G (b), and F4/80 (c) from the skin of mice treated with vehicle or nano-chitin 7 days after wounding (original magnification \times 400; Scale bar = 50 μ m). Topical application of nano-chitin significantly promoted wound vascularity (CD31) and neutrophil infiltration (Ly6G). Topical application of nano-chitin seemed to promote macrophage infiltration (F4/80), but the difference was not significant (n = 5 per group, * P < 0.05 vs. vehicle). hpf: high power field.

lation of IL-8 (Fig. 4C g) and bFGF (Fig. 4C h) in chitin-treated wounds was higher than that in saline-treated wounds (n = 4 per group, *P <

0.05, **P < 0.001 vs. control). In addition, IL-8 (Fig. 4D k) and bFGF (Fig. 4D l) expression decreased with time in the presence of nano-

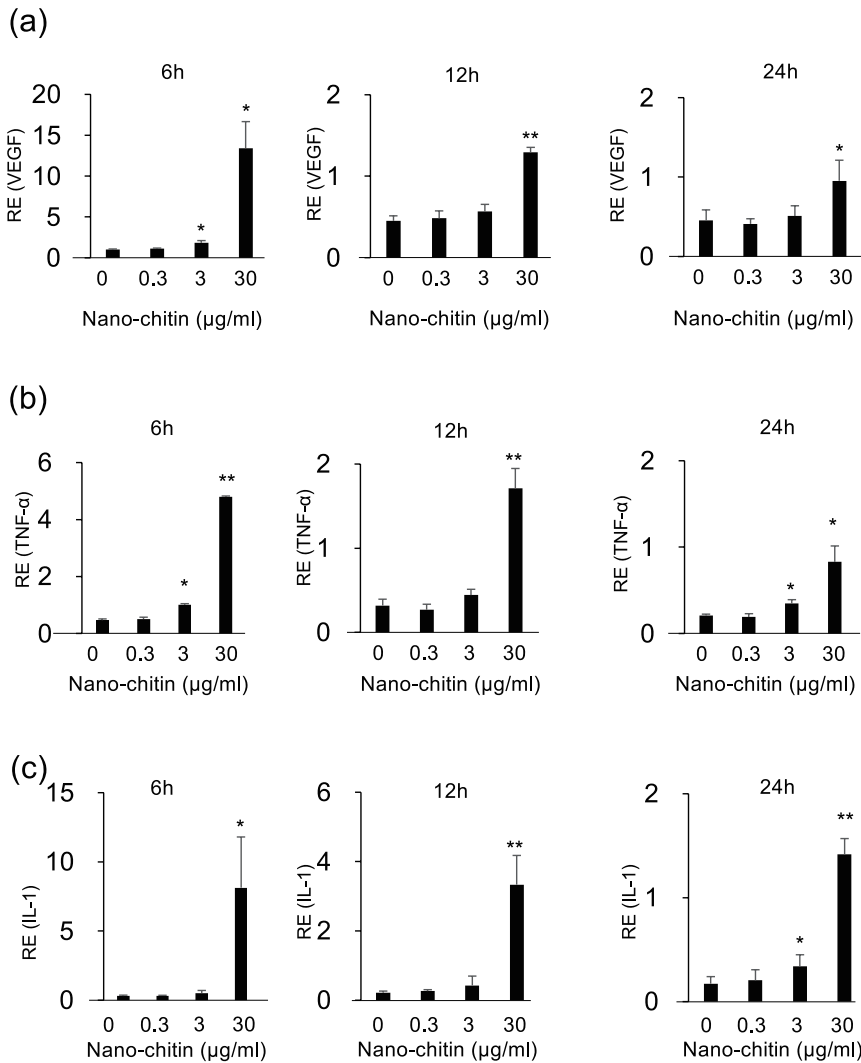


Figure 4A, 4B, 4C, 4D. Effects of nano-chitin on VEGF, TNF- α , IL-1, IL-6, IL-8, EGF and bFGF expression in THP-1 cells in vitro. Relative expression (RE) of VEGF, TNF- α , IL-1, IL-6, IL-8, EGF and bFGF mRNAs were evaluated using quantitative real-time RT-PCR, with normalisation to the control 18S rRNA. Nano-chitin upregulated VEGF (a), TNF- α (b), and IL-1 (c) mRNA levels in THP-1 cells in a dose-dependent manner. In addition, at all chitin concentrations, VEGF (d), TNF- α (e), and IL-1 (f) expression was highest after 6 h and decreased with time (n = 3 per group, *P < 0.05, **P < 0.001). And nano-chitin upregulated IL-8 (h) and bFGF (j) mRNA levels in THP-1 cells (n = 4 per group, *P < 0.05, **P < 0.001). In this study, nano-chitin did not upregulate IL-6 (g), and EGF (i). IL-8 (k) and bFGF (l) expression decreased with time in the presence of nano-chitin 30 μ g/ml (n = 3 per group, *P < 0.05).

chitin 30 μ g/ml (n = 3 per group, * P < 0.05).

Nano-chitin does not promote cell proliferation

To evaluate the effects of nano-chitin on proliferation and cytotoxicity, a proliferation assay with THP-1 cells was performed. The nano-chitin did not promote cell proliferation at any of the concentrations (0.3, 3, and 30 μ g/ml) and time points (6, 12, and 24 h) (Fig. 5) (n = 3 per group). Moreover, it did not inhibit the growth of

THP-1 cells even at higher concentrations (30 μ g/ml).

Comparison between nano-chitin and Beschitin®

Next, the effects of nano-chitin and Beschitin® on wound closure were compared. Full-thickness skin wounds were created on the dorsal skin of db/db mice and applied nano-chitin (3 mg) or Beschitin® (9.5 mg) immediately after wounding. Wound areas of nano-chitin- or

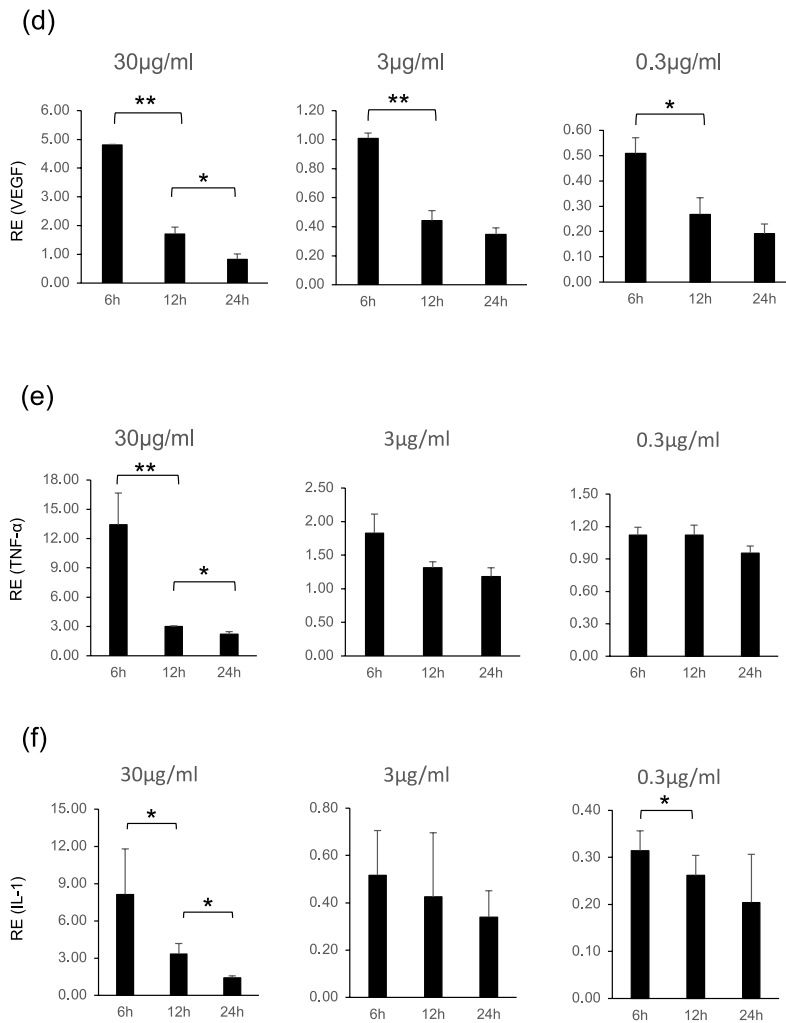


Figure 4B

Beschitin[®]-treated diabetic mice are shown in Fig. 6a. There were no significant differences between the effects of the two on days 4 and 7 (Fig. 6b). Histopathological studies showed that on day 7, there was no significant difference in the areas of granulation tissues in nano-chitin- and Beschitin[®]-treated groups (Fig. 6c and d).

Discussion

This study clarified that nano-chitin accelerated diabetic wound healing by promoting cellular infiltration, angiogenesis, and granulation tissue formation. *In vitro* experiments showing that nano-chitin upregulated VEGF and inflammatory cytokines in THP-1 cells endorse the stimulatory effects of chitin on impaired wound healing. To

consider the mechanism underlying the effects of nano-chitin on diabetic wound healing, Toll-like receptor 2 would be a plausible target. The expression of Toll-like receptor 2 is reportedly increased in type 2 diabetes, and Toll-like receptor 2 is involved in the activation and suppression of immune cells. In addition, chitin directly binds to Toll-like receptor 2 and activates immune cells, suggesting that applying nano-chitin to diabetic skin ulcers may induce inflammation via Toll-like receptor 2 and contribute to wound healing.^{15,16)} Wound healing is a dynamic interactive process with three phases-inflammation, granulation tissue formation, and tissue remodelling-that overlap in time.¹⁷⁾ In the initial inflammatory phase, inflammatory cells, such as neutrophils and

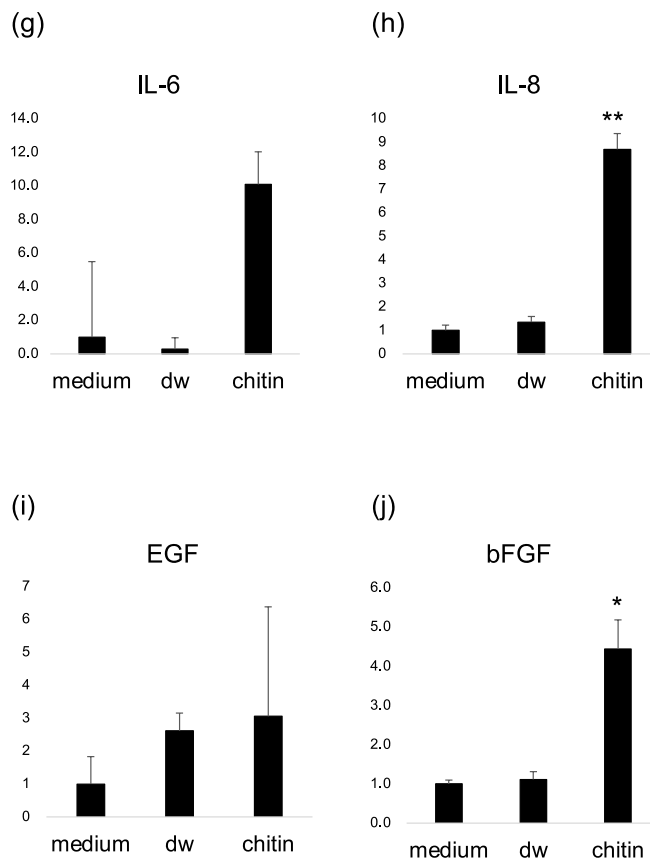


Figure 4C

macrophages, are recruited to the wound area by several chemotactic factors released by coagulation and activated parenchymal cells. Proinflammatory cytokines, such as IL-1 or TNF- α , produced by infiltrating neutrophils, activate monocyte/macrophage lineage cells to be the source of growth factors, including platelet-derived growth factors and VEGF, which initiate angiogenesis and granulation tissue formation. Several studies indicated that macrophages isolated from diabetic mice secrete reduced levels of inflammatory cytokines such as IL-1 β and TNF- α ,¹⁸⁾ and the reduced function of macrophages in diabetes is restored by IL-1 stimulation.¹⁰⁾ The stimulatory effects of nano-chitin on diabetic wound healing were thought to be mediated by restoring these inflammatory cytokines, which are essential to induce adequate inflammation to

accelerate cell infiltration and granulation tissue formation. In this study, the nano-chitin also upregulated VEGF in THP-1 cells that contributed to promoting angiogenesis.

In contrast to the significant differences between the vehicle and nano-chitin treatments on days 4 and 7, the differences between the two disappeared on day 10. This shows that the stimulatory effects of chitin were primarily due to the upregulation of inflammatory cytokines. The granulation tissue consists of inflammatory cells and fibroblasts. Fibroblasts produce an extracellular matrix and are gradually replaced by collagen fibres. When sufficient collagen fibres are formed, the wound healing process progresses to the tissue remodelling phase, and granulation tissues rich in inflammatory cells and fibroblasts are replaced by a relatively acellular scar. Cells in the

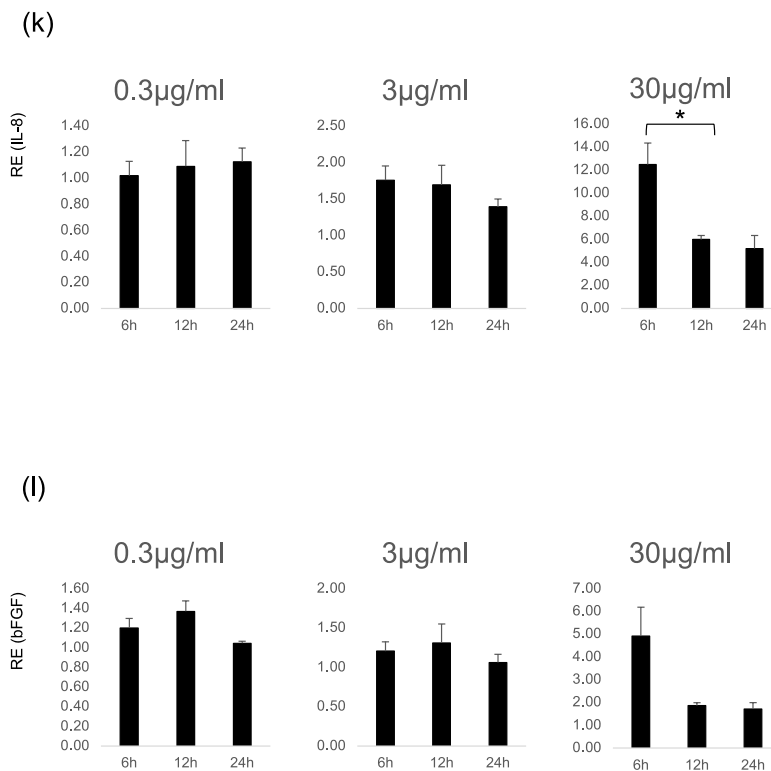


Figure 4D

wound undergo apoptosis.¹⁷⁾ Therefore, inflammatory cells are no longer needed at this phase, and excessive amount of inflammatory cells induced by nano-chitin is thought to be harmful for tissue remodeling. In this phase, excessive extracellular matrix (ECM) components such as fibronectin, proteoglycans, and collagens are degraded by matrix metalloproteinases (MMPs), contributing to normal wound repair.^{19,20)} There are several subtypes of MMPs. Of these, MMP-1, which is called collagenase 1, mainly cleaves type I collagen in cutaneous wound healing. When the balance between ECM production and degradation is disturbed, abnormal wound

healing occurs and leads to the formation of hypertrophic scars or keloids, which have a high amount of type I collagen rather than type III collagen.¹⁹⁾ Several previous studies reported the effects of chitin on fibroblasts and collagens in wound healing.^{21,23)} Kishimoto S, et al. indicated that the chitin membrane promoted deposition of type III collagen in the granulation tissue of wounds.²¹⁾ Lee KM, et al. showed that chitin derived from the cuttlebone extract induced the activation of fibroblasts, to increase the secretion of MMP-1, of which major ability at the wound is cleavage of type I collagen.²²⁾ These reports indicated that chitin could regulate quality and quan-

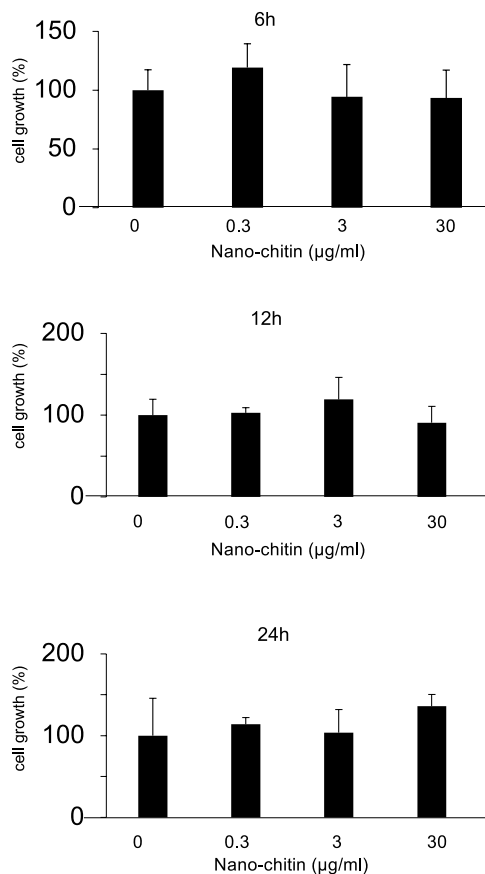


Figure 5. Effect of nano-chitin on THP-1 cell proliferation. Cytotoxicity of nano-chitin was evaluated using Cell Counting Kit-8. Nano-chitin did not promote cell proliferation at any of the concentrations and time points. (n = 3 per group)

tity of collagen in the wound to prevent abnormal scar formation such as keloid via the promotion of type III collagen synthesis and degradation of type I collagen by MMP-1. However, further studies are required to confirm this result.

According to the results of this study, nano-chitin should be used for chronic impaired wounds with little granulation tissue, which needs a trigger for initiating the inflammatory process of wound healing. The wounds with infection or necrotic tissues might also be appropriate since

inflammatory cells play a pivotal role in removing microorganisms and debris. In addition, I evaluated the effects of nano-chitin on proliferation and cytotoxicity. Nano-chitin does not inhibit cell growth, showing it can safely be applied for wound healing.

To date, chitin has been used in sheet form such as Beschitin[®], and past studies have shown that chitin is helpful as a wound dressing material.²⁰⁾²³⁾ However, these studies mostly accounted for *in vivo* experiments. This is the first study to

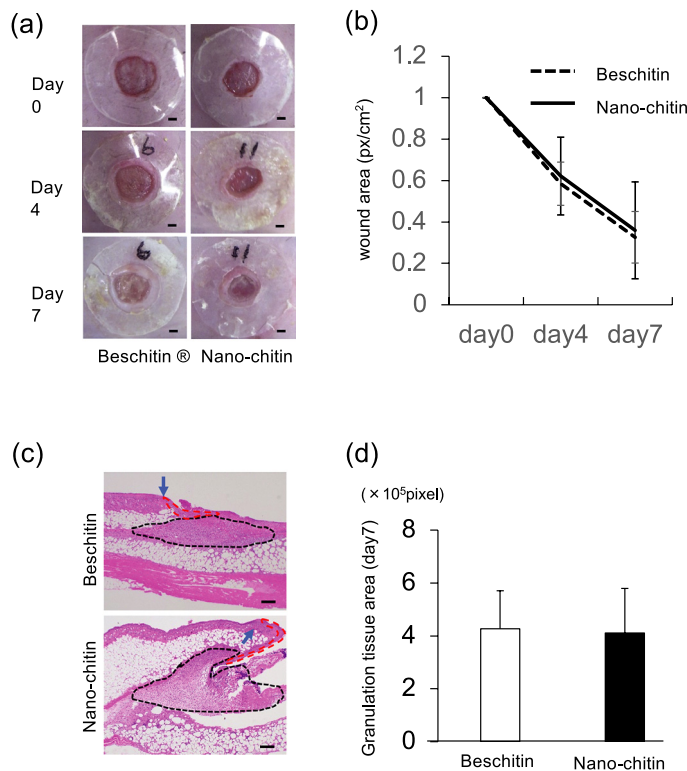


Figure 6. Effects of nano-chitin and Beschitin[®] on wound healing. Nano-chitin (3 mg) or Beschitin[®] (9.5 mg) was applied topically immediately after wounding. (a) Representative macroscopic appearance of the wound healing processes in the two treatment groups (left panels; Beschitin[®], right panels; nano-chitin). Scale bar = 2 mm. (b) Percentage of wound area on days 4 and 7. Nano-chitin-treated wounds showed about the same level of epithelialisation as Beschitin[®]-treated wounds (n = 10 per group). (c) Histological images (Hematoxylin and eosin staining, scale bar = 500 μ m) of the samples from the indicated groups. The black broken lines indicate the areas of granulation tissue, and the broken red lines indicate the newly-formed epithelium. Blue arrows indicate the original wound edge. (d) There was no significant difference in the granulation tissue areas between the nano-chitin- and Beschitin[®]-treated groups (n = 10 per group).

show the direct mechanism of the promoting effects of chitin on wound healing *in vitro*. I also evaluated the differences in the effects of nano-chitin and Beschitin®. Nano-chitin showed the same effect on wound closure as Beschitin®, which comprises three times higher chitin levels than the nano-chitin. The most important advantage of nanonisation would be increased surface area compared to fabric form. I speculated that this increased surface area due to nanonisation could make it easier to contact the cells. Furthermore, the gelatinous form of nano-chitin has another great advantage compared with the unsolvable crystalline structure in many respects. That is, the gelatinous compound can be applied to pocket-like ulcers and washed out, indicating its convenience in clinical use.

In conclusion, this study is the first report of soluble nanocrystal chitin, and confirms the

wound healing promoting effect of nano-chitin for the first time. To the best of my knowledge, this is also the first study to examine the effect of chitin *in vitro*.

Acknowledgements

I would like to thank K. Sato (Koyo Chemical Co., Ltd. Osaka, Japan) for preparing nano-chitin. I would also like to thank Prof. Norito Katoh, Dr. Jun Asai, and Dr. Takahiro Arita for the continuous supports and thoughtful guidance.

Funding

This study was funded by Nipro Corporation, Osaka, Japan.

Conflict of interest

The author indicated no potential conflict of interest.

References

- 1) Chen X, Yang H, Zhong Z, Yan N. Base-catalysed, one-step mechanochemical conversion of chitin and shrimp shells into low molecular weight chitosan. *Green Chem*, 19: 2783-2792, 2017.
- 2) Oura T, Minagawa H. Clinical trial of chitin wound protective texture (Beschitin®-W). 1. Results of multi-institutional control test in Hokkaido. *Nishi Nihon Hifuka*, 54: 998-1004, 1992.
- 3) Parada RY, Egusa M, Aklog YF, Miura C, Ifuku S, Kaminaka H. Optimization of nanofibrillation degree of chitin for induction of plant disease resistance: Elicitor activity and systemic resistance induced by chitin nanofiber in cabbage and strawberry. *Int J Biol Macromol*, 118 (Pt B): 2185-2192, 2018.
- 4) Sun C, Fu D, Jin L, Chen M, Zheng X, Yu T. Chitin isolated from yeast cell wall induces the resistance of tomato fruit to *Botrytis cinerea*. *Carbohydr Polym*, 199:341-352, 2018.
- 5) Bae MJ, Shin HS, Kim EK, Kim J, Shon DH. Oral administration of chitin and chitosan prevents peanut-induced anaphylaxis in a murine food allergy model. *Int J Biol Macromol*, 61:164-168, 2013.
- 6) Tripathi S, Mehrotra GK, Dutta PK. Physicochemical and bioactivity of cross-linked chitosan-PVA film for food packaging applications. *Int J Biol Macromol*, 45: 372-376, 2009.
- 7) Deepthi S, Venkatesan J, Kim SK, Bumgardner JD, Jayakumar R. An overview of chitin or chitosan/nano ceramic composite scaffolds for bone tissue engineering. *Int J Biol Macromol*, 93 (Pt B): 1338-1353, 2016.
- 8) Sato K, Tanaka K, Takata Y, Yamamoto K, Kadokawa JI. Fabrication of cationic chitin nanofiber/alginate composite materials. *Int J Biol Macromol*, 91:724-729, 2016.
- 9) Jeffcoate WJ, Harding KG. Diabetic foot ulcers. *Lancet*, 361: 1545-1551, 2003.
- 10) Maruyama K, Asai J, Ii M, Thorne T, Losordo DW, D'Amore PA. Decreased macrophage number and activation lead to reduced lymphatic vessel formation and contribute to impaired diabetic wound healing. *Am J Pathol*, 170: 1178-1191, 2007.
- 11) Asai J, Takenaka H, Katoh N, Kishimoto S. Dibutyl cAMP influences endothelial progenitor cell recruitment during wound neovascularization. *J Invest*

- Dermatol, 126: 1159-1167, 2006.
- 12) Asai J, Takenaka H, Hirakawa S, Sakabe JI, Hagura A, Kishimoto S, Maruyama K, Kajiya K, Kinoshita S, Tokura Y, Katoh N. Topical simvastatin accelerates wound healing in diabetes by enhancing angiogenesis and lymphangiogenesis. *Am J Pathol*, 181: 2217-2224, 2012.
 - 13) Lerman OZ, Galiano RD, Armour M, Levine JP, Gurtner GC. Cellular dysfunction in the diabetic fibroblast: impairment in migration, vascular endothelial growth factor production, and response to hypoxia. *Am J Pathol*, 162: 303-312, 2003.
 - 14) Livak KJ, Schmittgen TD. Analyzing real-time PCR data by the comparative CT method. *Nat Protoc*, 3:1101-1108, 2008.
 - 15) Sepehri Z, Kiani Z, Nasiri AA, Kohan F. Toll-like receptor 2 and type 2 diabetes. *Cell Mol Biol Lett*, 21:2, 2016
 - 16) Fuchs K, Cardona GY, Wolz O, Herster F, Sharma L, Dillen CA, Täumer C, Dickhöfer S, Bittner Z, Dang TM, Singh A, Haischer D, Schlöffel MA, Koymans KJ, Sanmuganantham T, Krach M, Roger T, Le Roy D, Schilling NA, Frauhammer F, Miller LS, Nürnberger T, LeibundGut-Landmann S, Gust AA, Macek B, Frank M, Gouttefangeas C, Dela Cruz CS, Hartl D, Nr Weber A. The fungal ligand chitin directly binds TLR2 and triggers inflammation dependent on oligomer size. *EMBO Rep*, 19, 2018.
 - 17) Singer AJ, Clark RA. Cutaneous wound healing. *N Engl J Med*, 341: 738-746, 1999.
 - 18) Zykova SN, Jenssen TG, Berdal M, Olsen R, Myklebust R, Seljelid R. Altered cytokine and nitric oxide secretion in vitro by macrophages from diabetic type II-like db/db mice. *Diabetes*, 49: 1451-1458, 2000.
 - 19) Aramaki N, Izogai Z, Okabe K, Kishi K. Extracellular matrix in Keloids. *Sosyo*, 5: 51-55, 2014.
 - 20) Rohani MG, Parks WC. Matrix remodeling by MMPs during wound repair. *Matrix Biol*, 44-46:113-121, 2015.
 - 21) Kishimoto S, Tamaki K. Immunohistochemical and histochemical observations in the process of burn wound healing in guinea pig skin under chitin membrane dressing. *Hifuka Kiyou*, 82: 471-479, 2000.
 - 22) Lee KM, Shim H, Lee GS, Park IH, Lee OS, Lim SC, Kang TJ. Chitin from the Extract of Cuttlebone Induces Acute Inflammation and Enhances MMP1 Expression. *Biomol Ther (Seoul)*, 21: 246-250, 2013.
 - 23) Singh R, Shitiz K, Singh A. Chitin and chitosan: biopolymers for wound management. *Int Wound J*, 14: 1276-1289, 2017.

〈和文抄録〉

糖尿病マウスにおける創傷治癒に対するナノキチンの作用

金子 由 佳

京都府立医科大学大学院医学研究科皮膚科学

キチンは生体適合性に優れた天然ムコ多糖である。日本では創傷被覆材として臨床的に使用されている（ベスキチン®）。今回、キチンの可溶ナノ結晶形を生成し、マウスの糖尿病性創傷治癒モデルを使用し創傷被覆材としてその治療効果を評価した。ナノキチンは、肉芽組織形成を有意に促進し、血管新生および炎症細胞浸潤の増加を認めた。さらにナノキチンは、キチンが3倍量含まれているベスキチン®と同等の創傷治癒効果を示した。また、*in vitro*でTHP-1細胞において、ナノキチンは肉芽組織形成促進の重要な因子であるVEGF, TNF- α , およびIL-1を促進した。これらの結果は、創傷治癒に対するナノキチンの効果は、炎症細胞に対する直接的な影響によるものであることを示唆している。今回、新たにゲル状のナノキチンを生成し、糖尿病マウスモデルで創傷治癒促進を確認した。この研究においてキチンの創傷治癒に与える効果のメカニズムを評価することができたが、*in vitro*でキチンの創傷治癒促進効果におけるメカニズムを検討した報告は過去になく、本研究がはじめてである。

キーワード：キチン，創傷治癒，ナノ医療。